

Mesoscopic currents in coupled atomtronic ring ladders

Tobias Haug,¹ Luigi Amico,^{1,2,3} Rainer Dumke,^{1,4} and Leong-Chuan Kwek^{1,5,6,7}

¹Centre for Quantum Technologies, National University of Singapore, 3 Science Drive 2, Singapore 117543, Singapore

²CNR-MATIS-IMM & Dipartimento di Fisica e Astronomia, Via S. Sofia 64, 95127 Catania, Italy

³LANEF 'Chaire d'excellence', Université Grenoble-Alpes & CNRS, F-38000 Grenoble, France

⁴Division of Physics and Applied Physics, Nanyang Technological University, 21 Nanyang Link, Singapore 637371, Singapore

⁵MajuLab, CNRS-UNS-NUS-NTU International Joint Research Unit, UMI 3654, Singapore

⁶Institute of Advanced Studies, Nanyang Technological University, 60 Nanyang View, Singapore 639673, Singapore

⁷National Institute of Education, Nanyang Technological University, 1 Nanyang Walk, Singapore 637616, Singapore

(Dated: September 6, 2022)

Recent experimental progress have revealed Meissner and Vortex phases in low-dimensional ultracold atoms systems. Atomtronic setups can realize coupled ring ladders, while explicitly taking the finite size of the system into account. This enables the engineering of quantized chiral currents and phase slips in-between them. In particular, full control of the lattice configuration reveals a reentrant behavior of Vortex and Meissner phases. Our approach allows a feasible diagnostic of the currents' configuration through time of flight measurements.

The response of quantum coherent systems to an external perturbation may be implying subtle physical phenomena. A textbook example in this context is provided by the Meissner effect. Originally formulated in condensed matter, the Meissner effect explains how a superconductor (a phase coherent system) thicker than the penetration depth expels magnetic fields. In a so called type II superconductor, however, the magnetic field can penetrate the superconductor, but it must be organized in a lattice of flux tubes (Abrikosov Vortex lattice)[1, 2]. Indeed, such phenomenon is intimately related to the Anderson-Higgs mechanism in relativistic Yang-Mills theories, and recent efforts have been devoted to understand whether Abrikosov vortices can occur in the Higgs field[3].

Ultracold atoms confined in optical lattices allow us to study the above problem in a novel and fruitful way[4]. Specifically, ladder structures have been considered, in which ultracold bosonic atoms can tunnel between two one-dimensional chains. An artificial gauge field [5–7] mimics the external magnetic field implied in the Meissner effect. In this context the perfect 'diamagnetism' arises from currents flowing along the legs (chiral currents). Recently, many experiments of such systems have been realized [8–12] and the theory has been studied in[13–21]. It was understood, in particular, that the commensurate Meissner state undergoes a quantum phase transition to an incommensurate Vortex lattice. The interplay of interacting bosons with strong magnetic fields in a low-dimensional system and chiral edge currents akin to Meissner surface currents have been demonstrated.

To study the problem, here we are inspired by Atomtronics: optical circuits of very different spatial shapes and intensity for manipulation of cold atoms[22, 23]. Atomtronic quantum technology aims at devising a circuitry of a new type with atomic currents. At the same time, with closed confinements, it can enable a new platform of cold-atom quantum simulators to explore quantum many-body phases which are characterized by the current [24]. The Meissner/Vortex transition described above provides a striking example in which Atomtronics can demonstrate its full potential. In this paper, we study the physics implied by Meissner and Vortex phases

at the mesoscopic scale and in ladders with closed boundary conditions. We shall see that quantum phase slips[25–29] and flux quantization[30] play important roles in the physics of these system. The physical platform of the system will be provided by a specific Atomtronic device made of two coupled bosonic condensates confined in 'on-top' ring-shaped optical potentials[31, 32]. With our approach, we will explain: *i*) how the configuration of the current in the two phases are related to persistent currents flowing in the ring condensates; *ii*) how to measure the phases with absorption imaging of the condensate; *iii*) how the current configuration is related to the two-level system dynamics evidenced in[31, 32].

The Model– Two rings A and B with each L sites are coupled via the rungs. A sketch of the model is shown in Fig.1a. The Hamiltonian $\mathcal{H} = \mathcal{H}_A + \mathcal{H}_B + \mathcal{H}_{\text{int}}$ is given by

$$\begin{aligned}\mathcal{H}_A &= \sum_{m=1}^L \left(-te^{i\phi_A} \hat{a}_m^\dagger \hat{a}_{m+1} + \text{h.c.} \right) + \frac{U}{2} \hat{n}_m^a (\hat{n}_m^a - 1) \\ \mathcal{H}_B &= \sum_{m=1}^L \left(-te^{i\phi_B} \hat{b}_m^\dagger \hat{b}_{m+1} + \text{h.c.} \right) + \frac{U}{2} \hat{n}_m^b (\hat{n}_m^b - 1) \\ \mathcal{H}_{\text{int}} &= \sum_{m=1}^L -g \left[(1-w) \hat{a}_m^\dagger \hat{b}_m + w \hat{a}_m^\dagger \hat{b}_{m+1} \right] + \text{h.c.} . \quad (1)\end{aligned}$$

Operators \hat{a}_m (\hat{a}_m^\dagger) and \hat{b}_m (\hat{b}_m^\dagger) destroy (create) a boson at site m in ring A and B respectively and $\hat{n}_m^a \doteq \hat{a}_m^\dagger \hat{a}_m$ and $\hat{n}_m^b \doteq \hat{b}_m^\dagger \hat{b}_m$ are the particle number operators. The parameter t corresponds to the intra-ring coupling, g to the inter-ring coupling; w is a parameter accounting for the relative twist between the two rings (it is described in detail later on), U the on-site interaction and L the number of sites per ring. The operators are constrained by periodic boundary conditions for each ring $\alpha = \{a, b\}$ with $\hat{a}_{L+1} = \hat{a}_1$. An artificial gauge field \mathbf{A}_α is introduced through the Peierls substitution $t \rightarrow te^{i\phi_\alpha}$, where $\Omega_\alpha = \phi_\alpha L = \frac{q}{\hbar} \oint_C \mathbf{A}_\alpha \cdot d\mathbf{r}$ is the total flux threading each ring, and ϕ_α the phase acquired when tunneling between neighboring sites. The artificial gauge field plays the role of a physical rotation imparted to the ring condensate [6]. The phase term

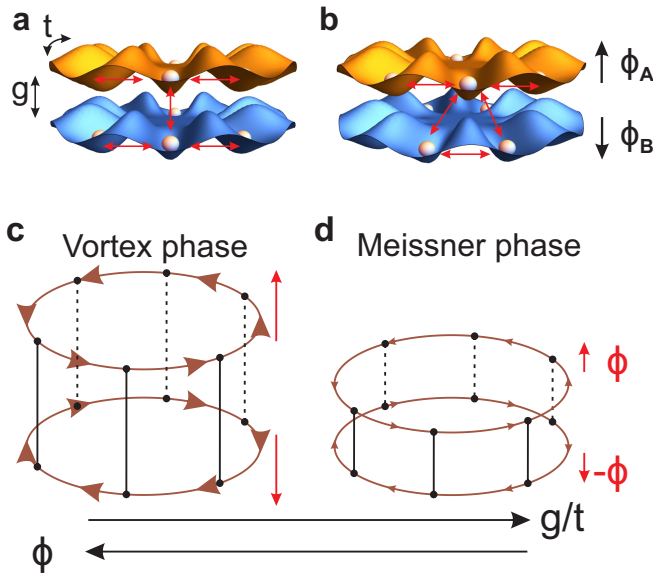


FIG. 1. Two on-top rings with local bosonic excitations at discrete sites. Bosons can tunnel to the nearest neighbors in the ring as well as to sites on the other ring. Rings may be twisted in respect to each other to shift relative position of sites. Upper and lower ring are threaded by a flux. In **a**, ring sites are aligned and inter-tunneling occurs between adjacent sites. In **b**, rings are twisted relative to each other, such that a site on ring A couples equally to two sites on ring B. The result is a triangular lattice. The red arrows indicate the possible tunneling between lattice sites. **c** When inter-ring coupling g/t is weak, or a high flux ϕ with opposite direction in each ring is applied: Two opposite and nearly uncorrelated currents in each ring (Vortex phase). **d** When rings are brought closer together to increase coupling, or flux is decreased: Rings resist external flux and acquire coherent phase with vanishing current (Meissner phase).

can be moved to the inter-ring coupling with the transformation $\hat{\alpha}_m \rightarrow \hat{\alpha}_m e^{-im\phi_a}$ [33, 34]. This transformation corresponds to a change from rotating to non-rotating reference frame.

The Hamilton can be solved exactly for $U = 0$ [19]. The phase winding in the ring is quantized to an integer phase winding number $n = \frac{1}{2\pi} \oint_C \nabla \Theta d\mathbf{r}$ [35] and represents a topological quantity which is associated with the persistent current [36].

We now return to the ring-twist parameter w mentioned in Eq. 1. This parameter is introduced in view of the new perspectives opened up by the Atomtronics quantum technology. The case $w = 0$ corresponds to the situation in which the two ring lattices are aligned vertically and the tunneling occurs only between neighboring sites in ring A and B (see Fig. 1a). Such instance defines a rectangular ladder. Alternatively, for $w = 0.5$ a site on ring A is in the plane in the middle of two sites on ring B, coupling a site on ring A equally to two sites on ring B. Such configuration defines a triangular ladder (see Fig. 1b and also [37–39]). Both rectangular and triangular ladder configurations may be realized by Laguerre-Gauss beams as outlined in [32]. A generic ring-twist w could be created with holographic methods[40].

Configuration of currents– We define the average current in the non-rotating laboratory frame [41]

$$j^{\alpha,\text{lab}} = -\frac{it}{L} \sum_{m=1}^L (\hat{\alpha}_m^\dagger \hat{\alpha}_{m+1} - \hat{\alpha}_{m+1}^\dagger \hat{\alpha}_m). \quad (2)$$

We consider opposite flux in each ring $\phi = \phi_A = -\phi_B$, which features the Meissner-Vortex transition mentioned in the introduction. It can be characterized by the chiral current $j_c = j^{A,\text{lab}} - j^{B,\text{lab}}$, which is the difference of the currents in ring A and B. A sketch of the configuration and currents is shown in Fig. 1c. For small inter-ring coupling g/t or large flux per site ϕ , the bosons in the two rings are effectively decoupled and rotate independently of each other, resulting in a large chiral current. The Vortex phase is defined by the ground state being the superposition of two degenerate states with counter-rotating angular momentum[16, 42]. In the other limit with large g/t or small ϕ , the inter-ring tunneling locks the phase of the bosons in both rings. As a result, the bosons coherently cooperate, stop rotating and the chiral current vanishes. With the logic of the perfect diamagnetism of the Meissner effect in superconductors, the resulting phase-locked condensates oppose the external flux driving the current.

Note that in Refs [8, 14, 43], the rotating frame is used to calculate the chiral current, which results in different values for the current, e.g. Meissner has maximal current and Vortex diminishing current. The general properties of the transition, of course, are independent of the frame, but the observables may be. We will consider the chiral current in the lab-frame as an order parameter. This parameter vanishes in the Meissner phase and acquires a finite value in the Vortex phase.

The Vortex/Meissner phases– First, we consider the Meissner-Vortex transition for a very large number of sites so that the effect of the periodic boundary conditions can be disregarded. The phase diagram is presented in Fig. 2. For the rectangular ladder ($w = 0$), we find a symmetry around $\phi = \pi/2$, which is broken for $w \neq 0$ (see Fig. 2a). For $g/t \ll 1$ or $\phi < \pi/2$, the phase diagram is nearly independent of ring-twist w . Remarkably, a transition can be induced by changing w . In particular, for $\phi > \pi$ and $w \approx 0.2$ a patch of Meissner phase is enclosed by the Vortex state. This area becomes larger with w . *Therefore a reentrant behaviour is found by increasing g for $\phi \approx 0.8\pi$.*

We plot the chiral current j_c for various cuts through the phase diagram for a large number of sites L in Fig. 3. In Fig. 3a, we plot j_c against inter-ring coupling g for different ring-twist configurations and $\phi = 0.8\pi$. While in a rectangular ladder, the current stops very quickly, for maximal ring-twist the Vortex phase extends to nearly $g/t = 8$. This is due to destructive interference of inter-ring tunneling in triangular configuration. For intermediate ring-twist $w = 0.2$ a reentrance is observed: With increasing inter-ring coupling, the chiral current goes to zero around $g/t \approx 3$. It reappears at intermediate couplings and then completely disappears for larger g/t .

In Fig. 3b the current is plotted against different degrees of ring-twist from rectangular ($w = 0$) to triangular ($w = 0.5$)

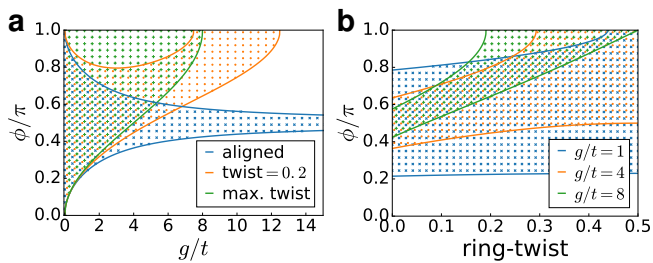


FIG. 2. The Meissner-Vortex phase diagram for flux per site ϕ . The Vortex phase is denoted by the dotted/crossed area. **(a)** Phase diagram with ϕ plotted against inter-ring coupling g/t for different values of ring-twist w . Diagram depends strongly on ring-twist for $\phi > 0.5\pi$. It shows a reentrant behaviour between the phases along the g/t axis for intermediate ring-twist and $\phi \approx 0.8\pi$. **(b)** Phase diagram plotted against w for different values of g/t . For $g/t = 8$ and flux $\phi \approx 0.8\pi$, increasing ring-twist shows the reentrant behaviour by passing Meissner-Vortex-Meissner phases.

configurations. Depending on inter-ring coupling and flux, twisting the ring configuration controls the current as well as drives phase transitions. For $g/t = 8$ and $\phi = 0.8\pi$ twisting reveals again the characteristic reentrant behavior, which drives a Meissner-Vortex-Meissner transition.

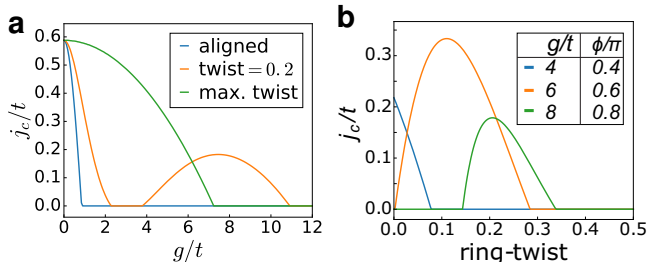


FIG. 3. **(a)** Chiral current j_c for a large number of sites L plotted against inter-ring coupling g/t and flux per site $\phi = 0.8\pi$. For $w = 0.2$, reentrance of the current is observed. **(b)** Chiral current plotted against ring-twist for different values of g/t and ϕ .

Next, we want to investigate the effect of a finite number of lattice sites L on the ground state current for the aligned configuration. For small L , j_c is not a monotonous function anymore, but changes as a stair case. It is plotted in Fig. 4a against inter-ring coupling g/t for various values of interaction U/t . The parameters are described in the caption. First, we discuss $U = 0$ which features sharp transitions. Such behaviour arises because of jumps between different values of angular momentum corresponding, in turn, to different winding numbers (a similar effect was evidenced in the Josephson current through a Luttinger liquid ring [44]). In between steps, the current does not define a plateau (strictly constant value between two steps). Instead, the current decreases with increasing inter-ring coupling or decreasing flux, which is explained in the following: In the Vortex phase, an equal number of bosons have positive and negative number of phase windings with same absolute value, say n and $-n$. In this case, the

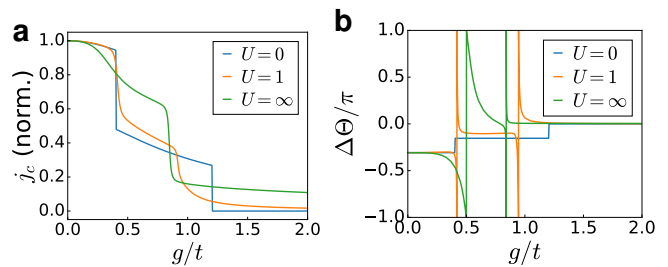


FIG. 4. **(a)** Ground state chiral current j_c vs inter-ring coupling g/t for finite $L = 13$ sites per ring, 6 particles and a total flux $\phi_A L = -\phi_B L = 3.2\pi$ for different values of interaction U/t . For $g = 0$, the rings are prepared with 2 (-2) phase windings in ring A (B). Current and phase winding decreases with g/t in two steps to nearly zero. With increasing U/t , second step appears at smaller g/t and transition smears out. **(b)** Phase jump of two point correlations $\Delta\Theta = \arg(\hat{a}_1^\dagger \hat{a}_7) - \arg(\hat{a}_1^\dagger \hat{a}_6)$ in ring A. Phase of ring B is identical with opposite sign. The transition between two different phase windings causes a change in phase by $2\pi(1 - 1/L)$.

system is prepared in a state with a topological phase winding $n = 2$ in ring A and $n = -2$ in ring B for $g = 0$. Then, the phase windings are well localized in either ring A (n) and B ($-n$). With increasing g , the phase windings begin to delocalize between the rings, decreasing the net chiral current. In the Meissner phase, the phase winding is completely delocalized, thereby suppressing j_c .

The scenario emerging from the above results indicates that the Meissner-Vortex phases transition in our system occurs because of quantum phase slips. In the Vortex phase, where the rings are effectively decoupled, upper and lower condensate have opposite phase winding. When increasing the inter-ring coupling, quantum phase slips occur between the opposing current states, which eventually cancel the phase winding difference in each ring to an average of zero.

Now we discuss the effect of non-zero interaction on the chiral current j_c . For all values of interaction a monotone decrease of the current with g/t is observed with two sharper drops. As explained above they mark the transition between current states with different integer phase windings. The smooth transition heralds the appearance of superposition states of different topological phase winding numbers. Fig. 4b reveals the phase jump of the two point correlations $\Delta\Theta = \arg(\hat{a}_1^\dagger \hat{a}_7) - \arg(\hat{a}_1^\dagger \hat{a}_6)$ in ring A. Phase for ring B has opposite sign. A change in phase of $\Delta\Theta = 2\pi(1 - 1/L)$ is observed whenever the ground state changes between two different phase windings. The actual value of $\Delta\Theta$ is determined by the superposition of phase windings[45].

With increasing interaction, the second step shifts from about $g/t \approx 1.2$ ($U = 0$) to $g/t \approx 0.84$ ($U = \infty$). This effect has been observed in [18] for ladders with open boundaries. While the Meissner state with zero phase winding has a negligible current, the Vortex state with non-zero phase winding consists of opposite current flows in ring A and B. These adverse flows scatter more strongly, thus having an increased energy compared to the resting Meissner state and making them

energetically less favorable.

Meissner/Vortex phases and the qubit dynamics– For sufficiently large L , the dynamics of the rectangular ladder system $w = 0$ was demonstrated to be governed by an effective two-level system for $\phi_A - \phi_B = \pi$ [31, 32]. Here, instead, we consider the currents configuration producing the qubit dynamics in a mesoscopic regime of moderate L and for the specific case $\phi_A = -\phi_B = \pi/2$. The energy gap is well defined for a wide parameter range. In the present mesoscopic regime, however, the first and second excited states are degenerate, which renders controlled addressing of only the two lowest levels as an effective qubit difficult. For this parameter regime, the system is always in a Vortex state and current flows clockwise (anti-clockwise) in ring A (B).

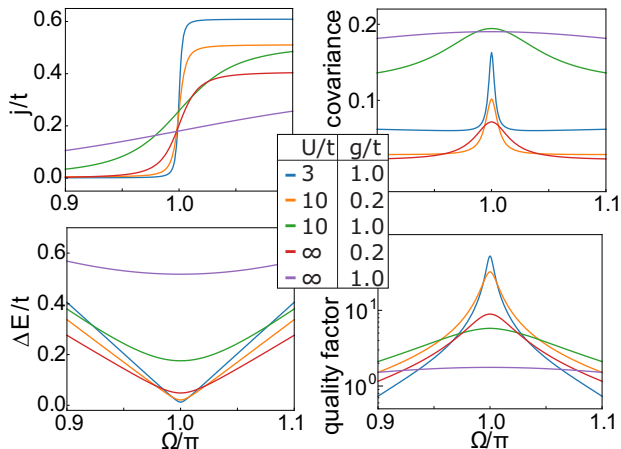


FIG. 5. Two coupled rings with 9 sites each and 9 particles threaded by the same total flux $\Omega = \phi_A L = \phi_B L$ for different values of interaction U/t and inter-ring coupling g/t . (a) Average current in lab-frame in either ring. (b) Covariance (a measure of correlation) of currents in ring A and B $\text{cov} = \langle j_A j_B \rangle - \langle j_A \rangle \langle j_B \rangle$. (c) energy gap ΔE between ground state and first excited state. (d) Quality factor Q , which is the ratio of energy difference of second excited state and first excited state, and ΔE . $Q > 1$ defines a good qubit. Further discussion of the qubit parameters is found in [46].

However, we find that $\phi_A L + \phi_B L = 2\pi$, $\phi_A L \approx \pi$ also defines a working point for a two level system. This configuration has been thoroughly studied for a single ring[46]. At the working point the states with zero and one phase winding hybridize as symmetric/anti-symmetric superpositions and an avoided crossing forms (see Fig.1 in [46]). Contrary to the single ring case, for two rings a finite gap appears even without a barrier when a half-filling particle number is chosen[35]. In Fig.5 the average current in either ring, current covariance, energy gap and quality factor (as defined in [46]) is studied in dependence of $\Omega = \phi_A L = \phi_B L$, for various values of interaction U/t and inter-ring coupling g/t . In Fig.5a, we observe a change from small to large average current across the optimal working point $\Omega = \pi$. At that point in Fig.5b, the current-current correlation (the so-called covariance) displays a positive maximum, which indicates that the two levels are now provided by co-propagating currents in the two rings.

We conclude that the effective two level system is an entangled NOON-state of both zero and one phase winding number, which is highly correlated between the rings.

Diagnostics– The current of the ultracold atoms confined

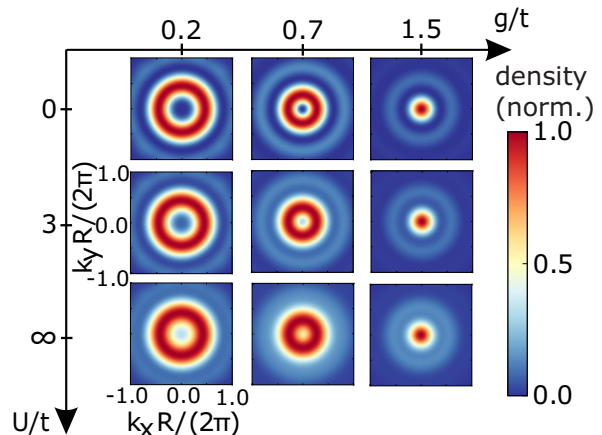


FIG. 6. Ground-state momentum distribution (time of flight) integrated along the inter-ring axis for different values of U/t and g/t for two rings with 12 sites each, 6 bosons and total flux $\phi_A L = -\phi_B L = 3.12\pi$. Details on the calculation are found in [46]. 2D graphs plot momentum k in XY -plane in units of ring radius R . The ratio R to the inter-ring distance is 5 : 3. The phase winding is proportional to the diameter of the central hole. By increasing g/t from left to right, the phase winding and hole decreases to zero in two quantized steps. With increasing interaction U/t , momentum distribution smears out.

in ring-shaped optical potential can be read out through time of flight experiments [24]. We exploit such a feature to tell apart Vortex and Meissner phases. Fig.6 shows the momentum distribution as a result of a time of flight experiment for different values of interaction and inter-ring coupling. The images plot the density integrated along the inter-ring axis. Chosen parameters are noted in the caption. The width of the annulus is proportional to the phase winding of the condensate, which only assumes integer multiples and is a measure for the current. From small to large coupling the number of phase windings changes from $n = 2$ ($n = -2$) in ring A (B) to $n = 0$. Interaction smears out the distribution, but the hole is still well visible. We show that time of flight experiments are a reliable way to determine the phase winding for two coupled rings. Observing the condensate from different angles or tracing the time-evolution of the expansion could realize a way to gain more information about the current distribution.

Conclusion– We studied the currents and the different physical regimes that can be established in a ring ladder at the mesoscopic scale, as provided by the Atomtronics quantum technology. The proposed system enables a feasible control of the relevant parameters of the system, implying an easy way to engineer current flows and quantum phase slips.

Because of the mesoscopic scale rings, quantized current steps are observed by tuning the inter-ring distance. With interaction, the steps reflect superpositions of different phase windings. The ring-twist w allows to vary continuously be-

tween rectangular and triangular ladder configurations (see Fig. 1a,b). As function of w , we found a reentrant behaviour in the Meissner-Vortex phase diagram and in the chiral current (see Fig. 2). We found a working point for which the system defines an effective qubit at the mesoscopic scale with co-rotating current configurations (see Fig. 5). Finally, we demonstrated with our approach that time-of-flight measurements provide a feasible way to expose the physics of the system implied in current and phase winding of the condensate (see Fig. 6).

Possible future work includes extending the ring ladder to three or more rings to study quantized edge currents analogue to the quantum Hall effect [9, 10]. The atomtronic two-ring setup could be used to study the supersolid phase [47]. The entanglement inherent to interacting bosons could be used to create a protocol for quantum enhanced rotation sensing [36]. In momentum space, the ring-twist realizes an interring coupling which depends on the quasi-momentum k with $g_k \propto 1 - w + we^{ik}$. For a particle with fixed k , we can identify each ring as an internal state of pseudo-spins [48]. Then, the twisted ring configuration could realize a nonlinear spin-orbit coupling to study new quantum phases.

Acknowledgements. We thank Anthony Leggett and Wenhui Li for enlightening discussions. The Grenoble LANEF framework (ANR-10-LABX-51-01) is acknowledged for its support with mutualized infrastructure.

-
- [1] W. Meissner and R. Ochsenfeld, *Naturwissenschaften* **21**, 787 (1933).
- [2] G. Rickayzen, in *RD Parks, Superconductivity* (Interscience, New York, Marcel Dekker, New York, 1969).
- [3] A. Sudbø, in *Superconductivity: Discoveries and Discoverers* (Springer, 2013) pp. 129–131.
- [4] I. Bloch, *Nat. Phys.* **1**, 23 (2005).
- [5] A. Eckardt, C. Weiss, and M. Holthaus, *Phys. Rev. Lett.* **95**, 260404 (2005).
- [6] J. Dalibard, F. Gerbier, G. Juzeliūnas, and P. Öhberg, *Rev. Mod. Phys.* **83**, 1523 (2011).
- [7] S. Tung, V. Schweikhard, and E. A. Cornell, *Phys. Rev. Lett.* **97**, 240402 (2006).
- [8] M. Atala, M. Aidelsburger, M. Lohse, J. T. Barreiro, B. Paredes, and I. Bloch, *Nat. Phys.* **10**, 588 (2014).
- [9] M. Mancini, G. Pagano, G. Cappellini, L. Livi, M. Rider, J. Catani, C. Sias, P. Zoller, M. Inguscio, M. Dalmonte, *et al.*, *Science* **349**, 1510 (2015).
- [10] B. Stuhl, H.-I. Lu, L. Ayccock, D. Genkina, and I. Spielman, *Science* **349**, 1514 (2015).
- [11] F. A. An, E. J. Meier, and B. Gadway, arXiv:1609.09467.
- [12] L. Livi, G. Cappellini, M. Diem, L. Franchi, C. Clivati, M. Frittelli, F. Levi, D. Calonico, J. Catani, M. Inguscio, *et al.*, arXiv:1609.04800.
- [13] A. similar ladder system has been studied with Josephson junctions in E. Granato, *Phys. Rev. B* **42**, 4797 (1990).
- [14] E. Orignac and T. Giamarchi, *Phys. Rev. B* **64**, 144515 (2001).
- [15] F. Crépin, N. Laflorencie, G. Roux, and P. Simon, *Phys. Rev. B* **84**, 054517 (2011).
- [16] A. Tokuno and A. Georges, *New J. Phys.* **16**, 073005 (2014).
- [17] S. Greschner, M. Piraud, F. Heidrich-Meisner, I. McCulloch, U. Schollwöck, and T. Vekua, *Phys. Rev. Lett.* **115**, 190402 (2015).
- [18] M. Piraud, F. Heidrich-Meisner, I. P. McCulloch, S. Greschner, T. Vekua, and U. Schollwöck, *Phys. Rev. B* **91**, 140406 (2015).
- [19] A. Keleş and M. Oktel, *Phys. Rev. A* **91**, 013629 (2015).
- [20] M. Di Dio, R. Citro, S. De Palo, E. Orignac, and M.-L. Chiofalo, *Eur. Phys. J. Special Topics* **224**, 525 (2015).
- [21] E. Orignac, R. Citro, M. Di Dio, S. De Palo, and M.-L. Chiofalo, *New J. Phys.* **18**, 055017 (2016).
- [22] B. Seaman, M. Krämer, D. Anderson, and M. Holland, *Phys. Rev. A* **75**, 023615 (2007).
- [23] L. Amico and A. M. G. Boshier, in *R. Dumke, Roadmap on quantum optical systems*, Vol. 18 (Journal of Optics, 2016) p. 093001.
- [24] L. Amico, A. Osterloh, and F. Cataliotti, *Phys. Rev. Lett.* **95**, 063201 (2005).
- [25] K. Matveev, A. Larkin, and L. Glazman, *Phys. Rev. Lett.* **89**, 096802 (2002).
- [26] G. Rastelli, I. M. Pop, and F. W. Hekking, *Phys. Rev. B* **87**, 174513 (2013).
- [27] I.-M. Pop, I. Protopopov, F. Lecocq, Z. Peng, B. Pannetier, O. Buisson, and W. Guichard, *Nat. Phys.* **6**, 589 (2010).
- [28] O. Astafiev, L. Ioffe, S. Kafanov, Y. A. Pashkin, K. Y. Arutyunov, D. Shahar, O. Cohen, and J. Tsai, *Nature (London)* **484**, 355 (2012).
- [29] T. Roscilde, M. F. Faulkner, S. T. Bramwell, and P. C. W. Holdsworth, *New J. Phys.* **18**, 075003 (2016).
- [30] K. C. Wright, R. B. Blakestad, C. J. Lobb, W. D. Phillips, and G. K. Campbell, *Phys. Rev. Lett.* **110**, 025302 (2013).
- [31] L. Amico, D. Aghamalyan, F. Auksztol, H. Crepez, R. Dumke, and L. C. Kwek, *Sci. Rep.* **4** (2014).
- [32] D. Aghamalyan, L. Amico, and L. C. Kwek, *Phys. Rev. A* **88**, 063627 (2013).
- [33] A. Osterloh, L. Amico, and U. Eckern, *Nucl. Phys. B* **588**, 531 (2000).
- [34] L. Amico, A. Osterloh, and U. Eckern, *Phys. Rev. B* **58**, R1703 (1998).
- [35] V. A. Kashurnikov, A. I. Podlivaev, N. V. Prokofev, and B. V. Svistunov, *Phys. Rev. B* **53**, 13091 (1996).
- [36] S. Ragole and J. M. Taylor, *Phys. Rev. Lett.* **117**, 203002 (2016).
- [37] T. Mishra, R. V. Pai, S. Mukerjee, and A. Paramekanti, *Phys. Rev. B* **87**, 174504 (2013).
- [38] E. Anisimovas, M. Račiūnas, C. Sträter, A. Eckardt, I. Spielman, and G. Juzeliūnas, arXiv:1610.00709.
- [39] S. Longhi, *Opt. Lett.* **39**, 5892 (2014).
- [40] T. Latychevskaia and H.-W. Fink, *Sci. Rep.* **6** (2016).
- [41] M. Cominotti, D. Rossini, M. Rizzi, F. Hekking, and A. Minguzzi, *Phys. Rev. Lett.* **113**, 025301 (2014).
- [42] R. Wei and E. J. Mueller, *Phys. Rev. A* **89**, 063617 (2014).
- [43] M.-C. Cha and J.-G. Shin, *Phys. Rev. A* **83**, 055602 (2011).
- [44] R. Fazio, F. Hekking, and A. Odintsov, *Phys. Rev. Lett.* **74**, 1843 (1995).
- [45] I. Danshita and A. Polkovnikov, *Phys. Rev. B* **82**, 094304 (2010).
- [46] D. Aghamalyan, M. Cominotti, M. Rizzi, D. Rossini, F. Hekking, A. Minguzzi, L. C. Kwek, and L. Amico, *New J. Phys.* **17**, 045023 (2015).
- [47] J. Li, J. Lee, W. Huang, S. Burchesky, B. Shteynas, F. Ç. Top, A. O. Jamison, and W. Ketterle, arXiv:1610.08194.
- [48] J. Li, W. Huang, B. Shteynas, S. Burchesky, F. Ç. Top, E. Su, J. Lee, A. O. Jamison, and W. Ketterle, *Phys. Rev. Lett.* **117**, 185301 (2016).